International Journal of Nanomedicine Dovepress

Open Access Full Text Article ORIGINAL RESEARCH

Green Synthesis and Characterization of Silver Nanoparticles Using *Zingiber officinale* Extracts to Investigate Their Antibacterial Potential

Muhammad Ramzan[1], Mai Abdel Haleem A Abusalah[2], Naveed Ahmed[3], Chan Yean Yean[3], Basit Zeshan[4]

[1]Department of Microbiology, Faculty of Science and Technology, University of Central Punjab, Lahore, 54000, Pakistan; [2]Department of Medical Laboratory Sciences, Faculty of Allied Medical Sciences, Al-Ahliyya Amman University, Amman, Jordan; [3]Department of Medical Microbiology and Parasitology, School of Medical Sciences, Universiti Sains Malaysia, Kubang Kerian, 16150, Malaysia; [4]Department of Microbiology, Institute of Industrial Biotechnology, Government College University, Lahore, Pakistan

Correspondence: Mai Abdel Haleem A Abusalah, Department of Medical Laboratory Sciences, Faculty of Allied Medical Sciences, Al-Ahliyya Amman University, Amman, Jordan, Email m.abusalah@ammanu.edu.jo; Basit Zeshan, Department of Microbiology, Institute of Industrial Biotechnology, Government College University, Lahore, Pakistan, Email basit.zeshan@gcu.edu.pk

Background and Purpose: Antimicrobial resistance (AMR) has emerged as a significant global concern. To combat this growing threat, various strategies have been employed, including the use of plant extracts and the biosynthesis of nanoparticles (NPs). The current study was designed to evaluate the phytochemical analysis of ginger (*Zingiber officinale*) extracts, characterize the silver nanoparticles (AgNPs) and to see their antibacterial potentials against multi-drug resistant (MDR) bacterial strains.

Methods: The extracts were prepared and initially assessed for their phytochemical composition and antibacterial activity. Then, AgNPs were synthesized from these extracts at room temperature, and various analytical techniques, including UV-visible spectroscopy, X-ray diffraction (XRD), ATIR-FTIR, zeta sizer, scanning electron microscopy (SEM), and energy-dispersive X-ray analysis (EDXA), were used to characterize the NPs. After confirmation of prepared NPs, they were subjected to their antibacterial activity.

Results: HPLC analysis demonstrated the presence of eight phytoconstituents in organic ginger extracts. The absorption spectra of the silver suspension exhibited surface plasmon resonance peaks with maxima between 420 and 448 nm. Functional groups like C-H, N-H, OH, C-O-C, C=O, and C-O were identified in both the organic and aqueous extracts of *Z. officinale*, playing a key role in the formation of AgNPs, as characterized by ATR-FTIR analysis. Both ginger organic and aqueous extract synthesized AgNPs crystalline structure was shown in XRD analysis and the particle size distribution showed average diameter of 200.5 nm of AgNPs from aqueous extracts. Scanning Electron Microscopy displayed spherical structure and EDA results showed the percentage of elements in synthesized AgNPs using plant extracts. Most promising antibacterial activity was obtained against *Escherichia coli ie* 20.83±0.53 for 100 µg/mL.

Conclusion: The results of the current study showed that AgNPs synthesized from different ginger extracts have promising antibacterial properties and can be potential candidates for alternative treatment options for bacterial infections.

Keywords: MDR pathogens, antibacterial activity, biosynthesized silver nanoparticles, ginger extract

Introduction

Green synthesis of silver nanoparticles (AgNPs) is an emerging strategy with profound consideration and progressive development in cutting-edge innovation and science. The importance of nanotechnology has been defined in broad industrial applications, such as in medical and engineering fields.[1,2] Most of the techniques used for preparation require the use of unsafe chemicals, long durations for the production of nanoparticles (NPs), and unfriendly environmental complications.[3,4]

The use of plants for the amalgamation of NPs has an edge over other biological strategies, as it does not require a longer harvest time for the reduction of metal ions.[5] Therefore, research has focused on biosynthetic green processes using plant extracts that are nontoxic and environmentally friendly.[6,7] Different factors, such as

Received: 26 April 2024
Accepted: 28 September 2024
Published: 11 December 2024

heat, pH, and time period, affect the various features of nanomaterials created from plant extracts. These extracts include phytoconstituents such as flavonoids, phenolics, and volatile oils, which have the ability to rearrange and maintain the functioning of AgNPs.[8] Phytochemicals, also known as bioactive metabolites, are naturally occurring substances that come from fruits, vegetables, herbs, and spices. Plant-based chemicals are considered key foundation materials for medication development in the pharmaceutical field.[9,10]

Bacterial organisms like *Klebsiella pneumoniae, Escherichia coli, Staphylococcus aureus, Salmonella species* and *pseudomonas species* have become resistant against most common commercially available antimicrobial agents.[11] The most common leading factor for antimicrobial resistance (AMR) in microbes is extensive misuse of antibiotics.[12] The emergence of AMR strains like is a worldwide challenge for clinicians and scientists. However, the plant bioactive compounds can be an alternative source for countering the prevalence of multidrug resistant microbes. In previous studies, it was proven that AgNPs exhibit strong antimicrobial activity.[13–15]

Ginger is among the medicines that have been most utilized since ancient times. It has numerous health advantages in addition to being used as a spice and flavoring ingredient.[16] Its pharmacological potentials have been thoroughly studied, including hepatoprotective, antibacterial, antioxidant, antinociceptive, anti-inflammatory, and antimutagenic potentials.[17] One of the most well-known plant families, *Zingiberaceae*, is frequently utilized as raw material for the making variety of traditional medicines.[18–20] *Zingiber officinale* (*Z. officinale*) could be the best source of secondary metabolites with therapeutic potentials, which is utilized in Chinese, ayurvedic, and unani medicines. These therapeutic effects are attributed to the presence of diverse volatile oils including sesquiterpenes, zingiberol, monoterpenes, and sesquiterpene hydrocarbons.[21] Zingberones, paradols, shogoals, and gingerdiols are significant phytoconstituents that have been extensively studied for their cardio-protective, immunomodulatory, anti-inflammatory, antioxidant, antihyperglycemic, and anticancer activities.[22]

Various antimicrobial medicines have been developed for the treatment of MDR bacterial infections.[23] Alongside the development of novel medicines, other treatment methods for bacterial infections are necessary to mitigate increased mortality rates. *Z. officinale* comprises many bioactive chemicals that serve as crucial capping and reducing agents. Consequently, it would be more advantageous to use the green synthesis of AgNPs. This work presents data on the manufacture of AgNPs using *Z. officinale'* extracts, both aqueous and organic. In the present work, both ginger extracts were first used for the biogenesis of NPs and then described. The antibacterial efficacy of *Z. officinale* ethanolic or organic extracts (ZOEE) and *Z. officinale* aqueous extracts (ZOAE) was evaluated against strains of *Staphylococcus aureus, Salmonella enterica*, and *Escherichia coli*.

Materials and Methods

Collection of Plant Samples

Fresh *Z. officinale* rhizome extract was collected from a local vegetable market in Lahore, Punjab, Pakistan, and was identified by Assoc. Prof. Dr. Abdul Nasir Khalid of the Department of Botany, University of the Punjab, Lahore (voucher # LAH-280922). After the collection of plant samples, these were shifted to the laboratory for proper cleaning with distilled water, and then shade-dried for a month. After the plant was allowed to dry in the shade, it was ground into a fine powder and stored in a zippered bag for further analysis (extraction).

Organic Extract Preparation from *Z. Officinale*

The plant material (25 g) was subjected to rigorous extraction using 250 mL of ethanol. The extraction was performed using a Soxhlet apparatus for a duration of eight hours at 70°C, and the extract was separated from the solid residue using filter paper. It was then placed in a refrigerator at 5°C after filtration and used in other experiments like for the AgNPs' synthesis. The filtrate was evaporated using a rotary evaporator for the biomedical analysis of the extracts and then secured in an airtight glass jar. Subsequently, the extract was stored in a refrigerator at 5°C until further experimentation.

Aqueous Extract Preparation from *Z. Officinale*

Ten grams of *Z. officinale* rhizome powder was isolated, added to a 100 mL distilled water flask and thoroughly mixed. This mixture was allowed to cool to room temperature after being heated in a water bath for 30 minutes at 35°C and then

filtered using Whatman filter paper. The filtrate was stored at 5°C for the next step in the synthesis of AgNPs, and some of it was evaporated in a rotary evaporator running at 40°C.[24] Once the remaining sample was carefully stored in a sealed container or glass bottle, it was refrigerated at 5°C. This ensured that the sample remained fresh and ready for future analyses, such as the screening and identification of the crude extract.

Preliminary Phytochemical Analysis

The preliminary screening for phytochemicals of the plant extracts was conducted to identify the presence of phytochemicals in organic or aqueous extracts of the rhizome *Z. officinale* such as phenolics, terpenoids, flavonoids, saponins, and alkaloids.[9]

High Performance Liquid Chromatography (HPLC) Analysis

HPLC analysis was conducted on *Z. officinale'* extracts to quantify eight specific standards, including myricetin, caffeic acid, benzoic acid, kaempferol, gallic acid, and sinapic acid. For this procedure, 5 mg of each standard and plant extract powder were dissolved in 2 mL of 95% ethanol, followed by filtration through a 0.45 µm syringe filter. The HPLC system utilized was an Agilent 1260 model (USA), equipped with a diode array detector (DAD) and a quaternary pump (1260). Data analysis was performed using ChemStation software. A filtered sample (20 µL) was injected into a reverse-phase (C18) Zorbax Eclipse Plus column (4.6 × 250 mm; 5 µm particle size, Agilent, USA). The mobile phase consisted of distilled methanol (solvent A) and 1% acetic acid (solvent B), with the following gradient (t in min; %A): (0 min; 60%), (5 min; 35%), (10 min; 10%), (15 min; 60%), and (20 min; 60%), at a flow rate of 1 mL/min in linear gradient mode. The column was maintained at a constant temperature of 25°C, and chromatograms were recorded at 280 nm. For flavonoid detection, two solvent systems were employed: solvent A (3% trifluoroacetic acid) and solvent B (acetonitrile, 80:20 v/v). These solvents were combined in a 50:50 v/v ratio, filtered under vacuum through a 0.45 µm membrane, and subjected to isocratic elution at 30°C with a flow rate of 1 mL/min. Detection was performed at a wavelength of 360 nm.[25,26]

Biosynthesis and Optimization of AgNPs Synthesis Condition

The ratio of rhizome *Z. officinale'* extracts to silver nitrate (AgNO3) solution (1:5), AgNO3 concentration (1 mm, 10 mm), pH (4.5, 6.5, 8.5, 10, 12), and incubation period (8h, 24h) were among the factors that were evaluated since they might influence NPs production. The reduction of silver ions to AgNPs was assessed through observable color changes, shifting from yellow to dark brown. The synthesis of *Z. officinale*-mediated AgNPs (ZO-AgNPs) was further confirmed using spectrophotometric analysis, conducted with a HALO DB-20/DB-20S spectrophotometer (Dynamica, Germany). After that, applications that produced tiny particle sizes of 27 µm were used to manufacture AgNPs,[27] which were thought to be ideal. AgNPs generated using ZOAE are called ZOAE-AgNPs, while those generated with ZOEE are called ZOEE-AgNPs.

Synthesis of NPs Using of *Z. Officinale*' organic and Aqueous Extract

$AgNO_3$ was prepared in aqueous form at concentrations of 1 and 10 mm before beginning the procedure. The synthesis of AgNPs was investigated using a spectrophotometer that relies on color change. AgNPs were created in accordance with previously reported processes, with slight modification.[27–30] For the bioreduction process, a 10 mm solution of $AgNO_3$ (125 mL) was gently mixed with ginger extract (25 mL) in a 500 mL glass bottle at room temperature. For 20 minutes, the mixture was shaken. Using a pH meter (Eutech Cyberscan pH 300), the reaction mixture's pH was quickly adjusted to pH 12, and it was then left in the dark for 24 hours to avoid photo-activation. Silver ion reduction was then observed based on the changes in color to reddish-brown or yellow. The synthesis of ZOEE-AgNPs and ZOAE-AgNPs was performed using spectroscopy. During the synthesis process, a 1 mL solution of ginger extract and $AgNO_3$ was used, which was then incubated with AgNPs. A 1 mL diluted suspension of AgNPs prepared with *Z. officinale* was mixed with distilled water and analyzed using a spectrophotometer. The spectrophotometer resolution was set at 0.5 nm, and absorbance was measured between 300 and 700 nm for 24 hours after the reaction started.

Purification of Prepared AgNPs

After incubation, to remove impurities,[31–33] the reddish-brown solution was centrifuged for 20 min at 6000 rpm. Hence, to remove non-essential enzymes or free proteins, the pellets obtained were cleaned twice using distilled water (5 mL) and once with 99% ethanol. The processed pellets were then placed in petri dishes and dried for 24 h at 60°C before use to test their biochemical features and properties against microbes.

Characterization of AgNPs Using X-Ray Diffraction Investigation

The powder samples were subjected to XRD (Model D8 Advance Bruker powder diffractometer, Bruker, Germany) at 20–80° with Cu Kα radiation (λ = 1.5406 Å) at 40 kV and 30mA to get the XRD profile of AgNPs.[34]

Characterization of AgNPs Using Scanning Electron Microscopy Attached with EDX Detector Analysis (SEM-EDXA)

Using a scanning electron microscope (Nova-Nano-SEM-450) running at 12 keV, the morphology of AgNPs generated by the aqueous or organic extracts was investigated. For elemental analysis, EDXA was used, and the presence of silver was confirmed precisely using SEM.[35]

Characterization of AgNPs Using ATR-FT-IR Analysis

Using FTIR (Bruker- alpha, V70, Pa Laiseau, France) measurements, the functional group in *Z. officinale* extract was identified, which played a role in stabilizing AgNPs. The fine powder of NPs and plant extract were analyzed using FTIR (in the region of 4000–500 cm^{-1}, transmittable mode with a resolution of 4 cm^{-1} and 50 scans).[34,35]

Determination of Zeta Potential and Particles Size

The particle size distribution was evaluated using dynamic light scattering, while the surface charge was measured with a Zeta Sizer Nano-ZS (Malvern Instruments Ltd., version 7.10, Malvern, Worcestershire, UK) according to a previously established protocol.[36]

Antibiotic Susceptibility of the Three Pathogenic Strains: (*S. aureus, Salmonella enterica* and *E. coli*)

Strains of *S. aureus, Salmonella enterica* and *E. coli* were used to test the antibacterial activity of the synthesized AgNPs according to the standard protocol outlined by Wayne (2012).[37] To obtain fresh and isolated colonies of bacterial strains, the bacterial samples were subcultured on nutrient agar and incubated for 24 hours at 37°C. The bacterial strains were taken from the University of Veterinary and Animal Sciences, Lahore's Microbiology Laboratory. After the incubation time, a battery of biochemical assays, such as coagulase, catalase, bile esculin, and DNA tests, were used to identify the bacterial colonies.[11]

The Kirby Bauer disk diffusion strategy was utilized to determine the antimicrobial activity of the bacterial strains following Wayne (2012)[37] and Altaf et al.[38] Agar plates were inoculated with 10 µL bacterial culture, and the surface was left to dry for 3 min. Antibiotic discs were then carefully placed on inoculated agar plates using sterile forceps. The plates were then incubated at 37°C for 24 h. After 24 h, the inhibition zone was measured using a ruler, and the standard deviation of the three measurements was calculated. MDR pathogens were defined as bacterial strains resistant to fewer than three antibiotics.[39] The antibiotic discs used in this study contained oxacillin, cloxacillin, amoxicillin (25 µg), azocillin (75 µg), and ticarcillin (75 µg).

Agar Well Diffusion Method

Agar plates were inoculated with 10 µL bacterial culture, and the surface was left to dry for 3 min. Later on, a diameter of 5 mm hole was created using sterile tips, and then a micropipette (50 µL) was used to collect 100 µg of *Z. officinale'* extract in 1 mL PBS and 100 µg ZO-AgNPs in 1 mL PBS in separate tubes. The experiment involved three replicates for each treatment, which were incubated for 24 h at 37°C. After the incubation period, the zone of inhibition was measured. The test was performed in triplicates to obtain the standard deviation of the measurements.

Estimation of MICs for Synthesized AgNPs

To 5 mL of Muller Hinton broth, 100 µL of biosynthesized AgNPs (Figure S1) using *Z. officinale'* organic and aqueous extracts (different concentrations like 100, 50, 25, 12.5.6.25, 1.56, 0.78, 0.39, 0.195, and 0.097 µg/mL) were added to different tubes, then twenty microliters of 1×10^6 CFU/mL *E. coli* culture were inoculated into two sets of different tubes, namely, A for ZOEE-AgNP and B for ZOAE-AgNPs. A separate test tube for positive control (medium and inoculum) and negative control (phosphate-buffered saline and medium) were used. The tubes were incubated for 24 h at 37°C. Before and after incubation, the absorbance was taken using a spectrophotometer at 630 nm (DB-20S). Following formula was used to calculate the values of each test tube:

Value = ODA –ODB.

ODA: after incubation.

ODB: before incubation.

The list of abbreviations used in the current study has been provided in Table S1.

Results

Phytochemical Analysis of Plant

The phytochemical ingredients were investigated qualitatively that were responsible for AgNPs capping and reduction in biogenic extracts of *Z. officinale*. Phytochemical screening of *Z. officinale* (organic and aqueous) revealed that neither ZOEE nor ZOAE contained alkaloids, flavonoids, or phytosterols. A large number of tannins, phenolic compounds, saponin glycosides, steroids, and triterpenoids are present.

HPLC Analysis

Comparing the organic extract of *Z. officinale* with the standard, the HPLC analysis revealed eight components that could be identified. Identification was achieved by comparing the retention times of phenolic and flavanol compounds to those of reference standards. The retention time of each analyte was used to select peaks that corresponded with the standards, ensuring accurate identification. The HPLC software can identify phenolic and flavonoid chemicals that exhibited peaks with retention times comparable to the standards. This gave each analyte's identification a foundation.

The *Z. officinale'* extract was found to contain several key components, including caffeic acid, gallic acid, sinapinic acid, kaempferol, quercetin, benzoic acid, chlorogenic acid, and myricetin. Chlorogenic acid (1.81%), gallic acid (2.56%), sinapinic acid (7.52%), caffeine (1.12%), myricetin (30.18%), benzoic acid (0.23%), kaempferol (0.44%), and quercetin (6.34%) in the ethanoic extract are the components from the family of phenolic compounds that have been found. Table 1 presents the results of the HPLC analysis of the *Z. officinale'* extract, revealing additional biomolecules as

Table 1 Flavonoid and Phenolic Contents in the *Z. Officinale* Rhizome Extract, Determined by the HPLC Methods

Plant Name	Phenolic and Flavonoid Compounds	Retention Time	Area%	Wavelength nm	mg/g
ZOEE	Benzoic acid	12.826	0.2307	280	0.045± 0.006
	Gallic acid	7.117	2.5695		0.173± 0.11
	Sinapinic acid	11.619	7.5296		0.016 ± 0.003
	Caffeic acid	10.23	1.1224		0.126 ± 0.05
	Chlorogenic acid	9.391	1.8186		0.021± 0.003
	Kaempferol	4.603	0.4445	360	0.053 ± 0.05
	Quercetin	3.424	6.3434		0.083 ± 0.14
	Myricetin	2.941	30.1837		0.267 ± 0.41

Table 2 Standard Flavonoid and Phenolic Constituents Determined by the HPLC Methods

Phenolic and Flavonoid Compounds	Retention Time	Wavelength (nm)
Benzoic acid	12.97	280
Gallic acid	7.03	
Sinapinic acid	11.58	
Caffeic acid	10.36	
Chlorogenic acid	9.37	
Kaempferol	4.46	360
Quercetin	3.51	
Myricetin	2.84	

indicated by extra peaks. Table 2 outlines the HPLC analysis of standard flavonoids and phenolic compounds. The peaks identified in the HPLC analysis of the various *Z. officinale'* extracts (both aqueous and organic) correspond to components such as chlorogenic acid, sinapinic acid, caffeine, myricetin, benzoic acid, kaempferol, and quercetin (Figures S2–S5).

Optimization AgNPs Using *Z. Officinale* Extracts by UV-Vis Spectrophotometer Analysis

Various experimental parameters were tested to determine the optimal biogenic synthesis of AgNPs. UV-Visible Spectra were recorded to observe the changes that occurred owing to the variations in the response parameters. Determining the parameters mentioned above is ideal for generating AgNPs.

Effect of pH on ZO-AgNPs Synthesis

When considering the impact of pH, it is important to focus on the most significant parameter affecting the arrangement of the NPs. Figure 1 illustrates the impact of the condition response on the synthesis of NPs and the pH of UV-vis spectra. The AgNPs' absorption bands were produced using *Z. officinale* extracts at different pH levels. The volume of

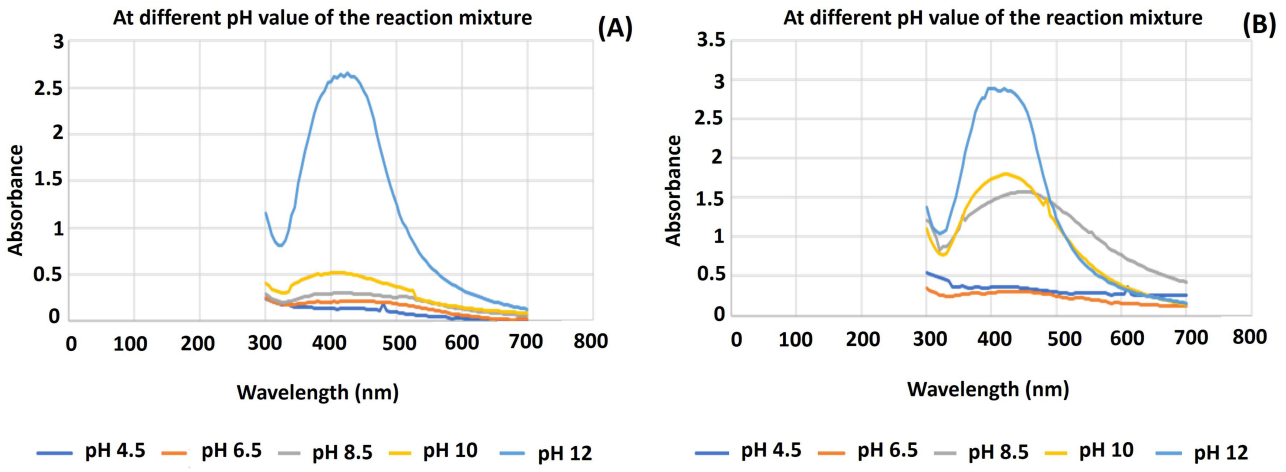

Figure 1 UV-Visible Spectra (**A**) variation of pH using ZOAE and 10 mm $AgNO_3$ aqueous solution reaction mixture for 24 h at ambient temperature and (**B**) variation of pH using ZOAE and 10 mm $AgNO_3$ aqueous solution reaction mixture reaction mixture at room temperature for 24 h.

the organic and aqueous plant extracts used was 25 mL, while the concentration of the aqueous $AgNO_3$ solution was 10 mm (125 mL). The incubation time and temperature were maintained at constant levels, with the temperature set to room temperature. The synthesis of NPs was highly efficient under alkaline conditions with a pH of 12. The intensity of plasmon absorbance bands increased as the pH ranged from 8.5 to 12, while these bands were either absent or significantly diminished at acidic pH levels. Additionally, at pH values between 6.5 and 12, the solution's color shifted from brown to dark or reddish brown within 24 hours of mixing the aqueous $AgNO_3$ solution with both extracts.

Effect of Reaction Time on ZO-AgNPs Synthesis

Figure 2 illustrates the effects of various factors on the biosynthesis of NPs, including the influence of incubation time. It also shows the UV-Vis absorption bands of AgNPs synthesized using *Z. officinale'* extracts at different incubation intervals. At different incubation durations, an absorption band was seen in the 400–480 nm region. Peak intensity peaked during a 48-hour period during which it steadily climbed. For 24 hrs, the stability of the NPs in suspension was monitored. The UV-VIS analysis verified that *Z. officinale* extracts, both aqueous and organic, reduced silver ions to AgNPs.

Effect of $AgNO_3$ Concentration

Figure 3 shows the impact of the concentration of AgNO3, the UV-VIS absorption bands of the produced AgNPs, and the observed impacts of the condition response on the biosynthesis of AgNPs. Different molar concentrations of the AgNO3 solution were used with extracts from the rhizome of *Z. officinale*, both organic and aqueous. The presence of a distinct surface plasmon resonance (SPR) peak within the visible spectrum, between 400 and 500 nm, indicated the successful formation of AgNPs. In contrast, this SPR peak was absent in the UV-Vis spectra of the $AgNO_3$ solution and the aqueous and organic extracts of *Z. officinale*. During the investigation of the impact of different concentrations of $AgNO_3$ (1 and 10 mm) on AgNP synthesis, it was observed that a higher concentration of $AgNO_3$ resulted in greater organization of AgNPs, as indicated by the high absorbance peak (Figure 3). The reaction mixture containing varying concentrations of $AgNO_3$ was examined using UV-VIS following a 24-hour incubation period at pH 12. Based on these findings, a concentration of $AgNO_3$ 10 mm is optimal for future investigations.

UV-Vis Spectroscopy for Optimized ZOEE-AgNPs and ZOAE-AgNPs

In order to obtain a suitable AgNP size, some conditions were optimized as follows: the prepared ginger extracts (aqueous 25 mL) were slowly mixed in a 500 mL glass bottle with a prepared 10 mm aqueous $AgNO_3$ solution (125 mL) for the reduction process and shaken for 20 min. To avoid photo-activation, the reaction mixture's pH was quickly adjusted to 12 using a pH meter and a 24-hour dark incubation period. The reduction of silver ions to NPs was identified by a color change to dark or reddish-brown. The formation of ZOAE-AgNPs was confirmed through spectroscopic analysis. An analogous procedure was employed to synthesize the AgNPs from the ZOEE-AgNPs.

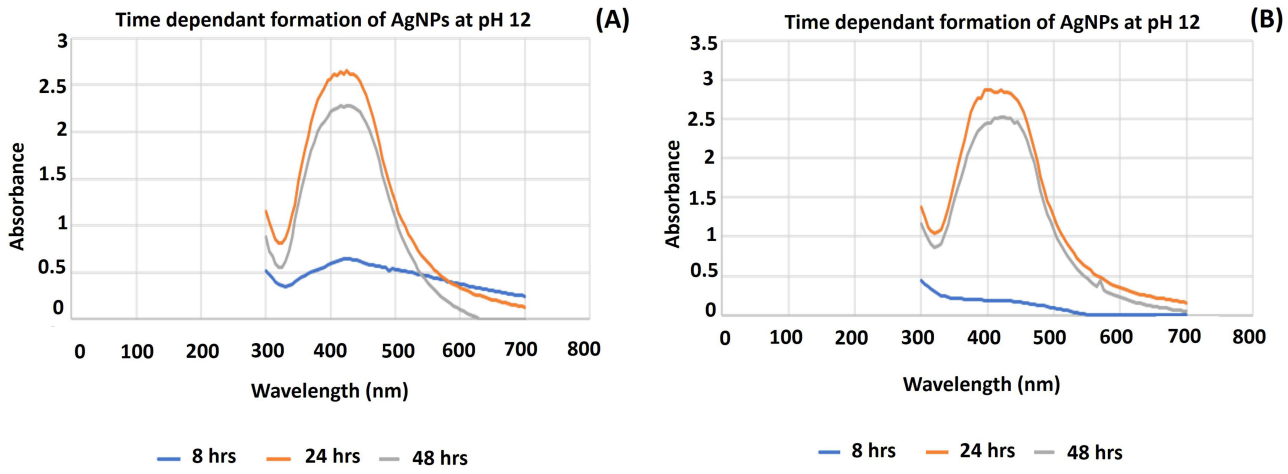

Figure 2 (**A**) UV-Visible Spectra of the time-dependent formation of AgNPs at pH 12 using ZOAE and 10 mm $AgNO_3$ aqueous solution reaction mixture. (**B**) UV-Visible Spectra of the time-dependent formation of AgNPs at pH 12 using ZOEE and 10 mm $AgNO_3$ aqueous solution reaction mixture.

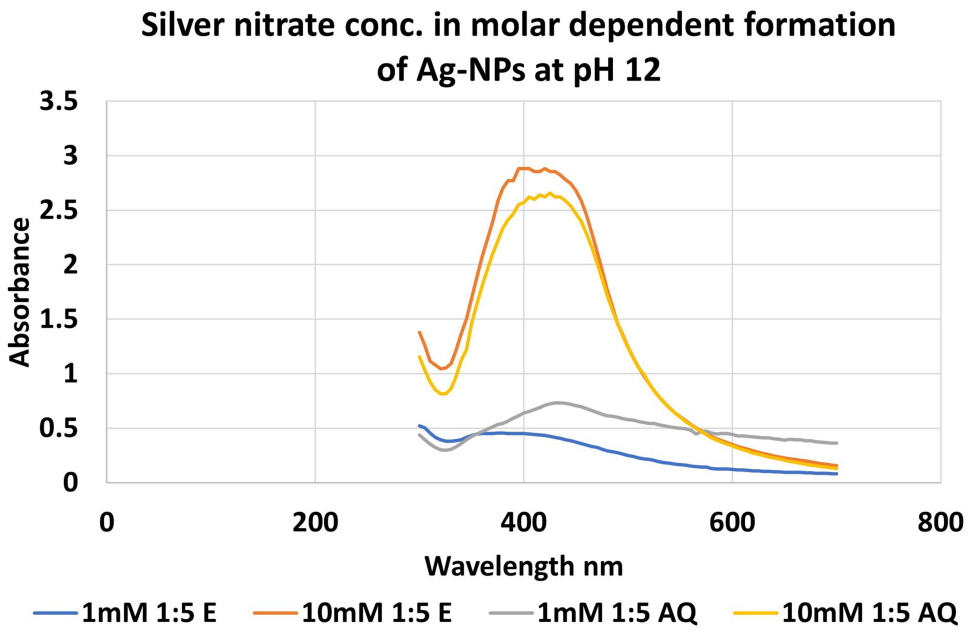

Figure 3 The formation of AgNPs was observed at pH 12 by using different molar concentrations of $AgNO_3$ aqueous solution and plant extract (ZOAE and ZOEE). The reaction mixture, consisting of 1 mL plant extract and 5 mL $AgNO_3$ solution, was kept at room temperature for 24 hours.

The reaction between the ginger extract and silver ions was observed by UV-Vis spectroscopy of the synthesized AgNPs. Spectroscopic analysis revealed the presence of an SPR peak at 420 nm for ZOEE-AgNPs and 425 nm for ZOAE-AgNPs (Table 3 and Figure 4). AgNP presence was confirmed by the observed UV-Vis spectroscopy band, which was caused by SPR absorption. Surprisingly, the NPs from ZOEE and ZOAE had very different maximum absorption wavelengths. This may be because the phytoconstituents from various sources interact with the biosynthesized AgNPs, causing varying interferences with the SPR absorption signature.

XRD Analysis

Figure 5 illustrates peaks at 2θ values ranging from 20° to 80°. In the *Z. officinale* rhizome' organic extract, the NPs peaks were observed at 27.80°, 32.25°, 38.12°, 46.13°, 54.64°, 57.15°, 64.26°, 67.46°, and 76.87°. In contrast, *Z. officinale'* aqueous extract displays peaks at 27.80°, 32.15°, 34.21°, 37.92°, 43.83°, 46.13°, 54.76°, 57.45°, 64.26°, 67.46°, and 77.07°. These findings indicate the crystalline nature of the NPs. The NPs that can be indexed as crystalline silver having peaks at 2θ value of 38.12°, 43.83, 64.26° and 77.07° to the (111, 200, 220 and 311) planes of the face-centered cubic structure, respectively, are shown in XRD pattern (JCPDS File: 00–024-0072). The 110, 111, 111, 200, 220, 220, and 311 planes of the face-centered cubic phase of silver oxide are shown in the XRD pattern at 2θ value of 27.80°, 32.15°, 32.25°, 37.92°, 54.76°, 54.64°, and 64.26° correspondingly (JCPDS File: 00–012-0793). To determine the size of silver oxide NPs, the maximum intensity peak is computed. The silver oxide extracts were picked at 111, 311 lattice plane. The average particle size for organic extracts of used silver was calculated to be 63.8nm using Debye Scherrer equation and 61.7 nm for aqueous extract of silver oxide.

Table 3 Absorbance and Wavelength of *Z. Officinale'* Synthesized AgNPs

Molar Concentration	PH	ZOEE-AgNPs Wave length (nm)	ZOEE-AgNPs Absorbance	ZOAE-AgNPs Wavelength (nm)	ZOAE-AgNPs Absorbance
1	12	379.0	0.457	430.0	0.733
10		420.0	2.883	425.0	2.657

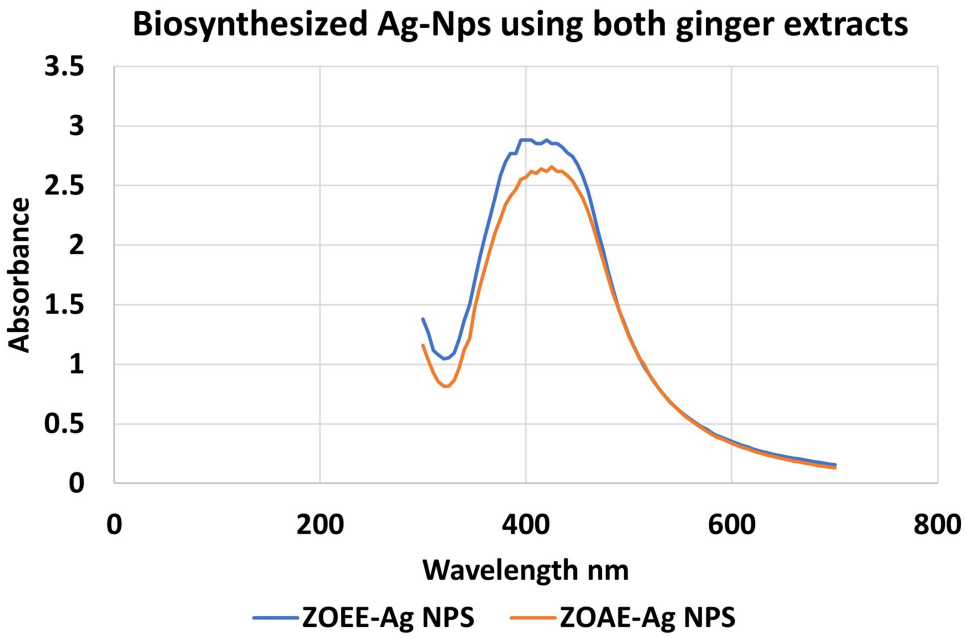

Figure 4 UV-Vis spectroscopy for ZOEE-AgNPs and ZOAE-AgNPs.

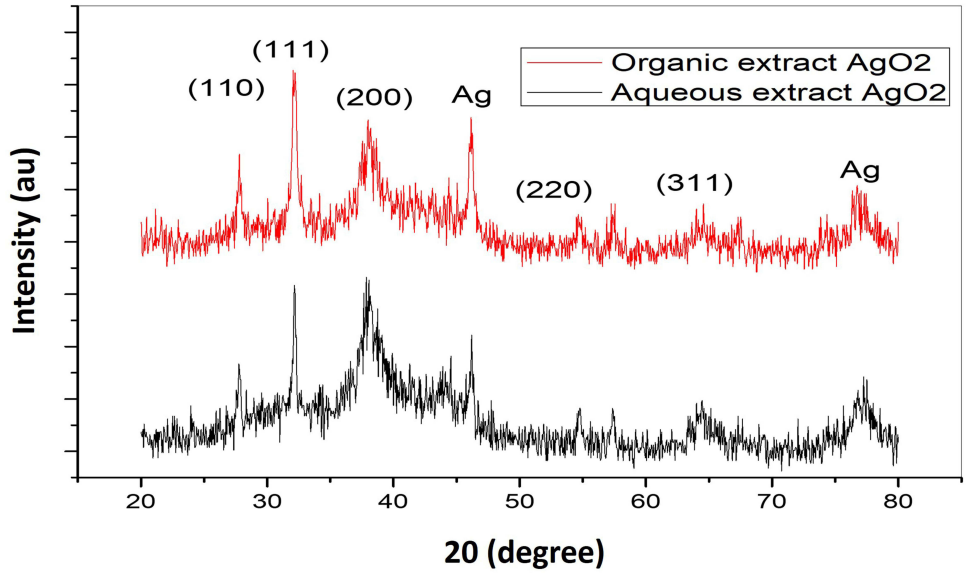

Figure 5 Synthesized AgNPs extract of *Z. officinale* XRD pattern (B= ZOEE-AgNPs, D=ZOAE-AgNPs).

Where,

D = average crystalline size,

K = dimensionless shape factor with a value close to unity (0.99).

λ= wavelength of cukα, (λ 1.54Å)

β = full width at half maximum of diffraction peaks, and

θ = Bragg's angle.

SEM and EDXA

The shapes of the prepared NPs were analyzed using SEM. SEM analysis (Figure 6) revealed a spherical shape, whereas SEM was coupled with EDX mapping to show the distribution of Ag, carbon, and oxygen in both the AgNPs (Figure 7

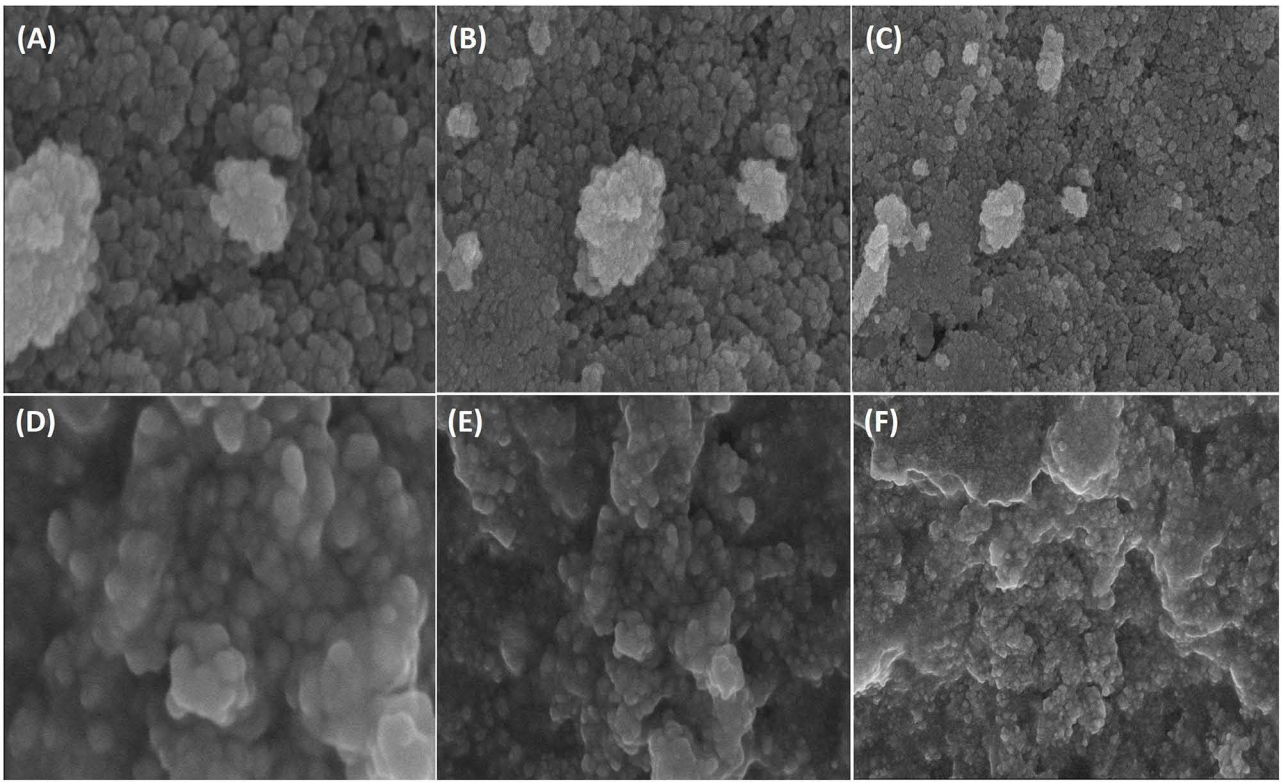

Figure 6 The shape of ZOAE and ZOEE synthesized AgNPs from at different magnification were shown through SEM micrograph. (**A**) ZOAE-AgNPs at magnification of 3,00,000× (100 nm). (**B**) ZOAE-AgNPs at magnification of 2,00,000× (200 nm). (**C**) ZOAE-AgNPs at magnification of 1,00,000× (500 nm). (**D**) ZOEE-AgNPs at magnification of 2,00,000× (200 nm). (**E**) ZOEE-AgNPs at magnification of 1,00,000× (500 nm). (**F**) ZOEE-AgNPs at magnification of 50,000× (1 µm).

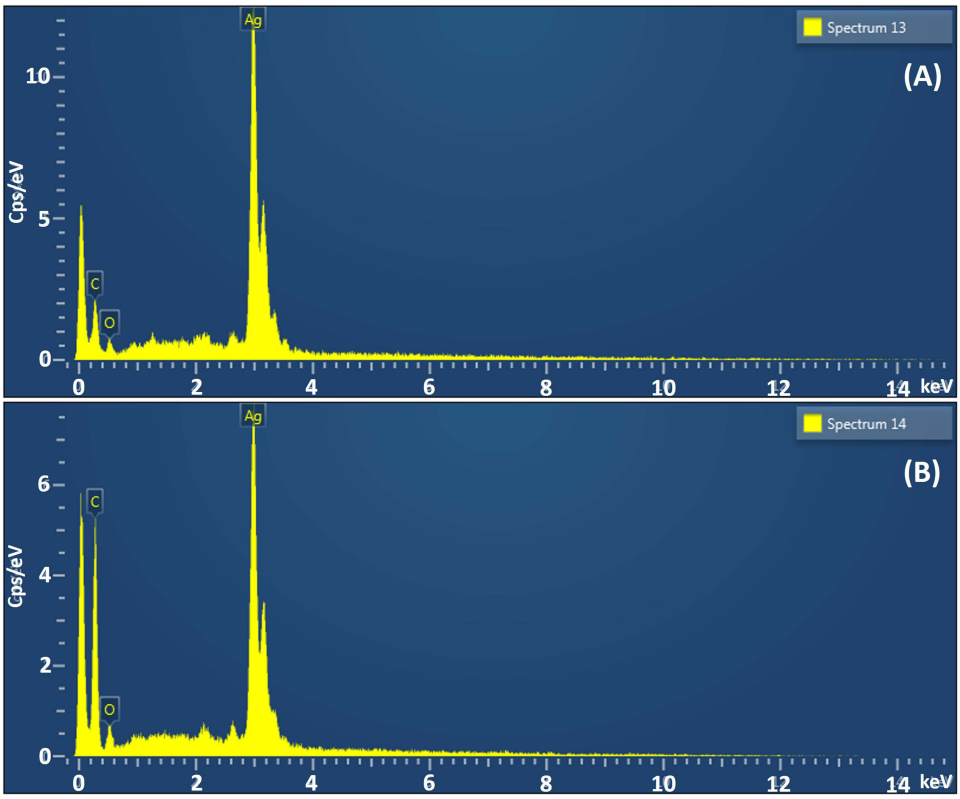

Figure 7 The quantitative amount of different element in the synthesized AgNPs were demonstrated using EDX spectra for extracts of *Z. officinale*. (**A**) ZOAE-AgNPs. (**B**) ZOEE-AgNPs.

and Table S2-S3). The results showed the presence of strong silver signals at 3KeV, as well as carbon and oxygen. It is clear from Table S2-S3 that the weight percentage of silver is 90.97% and 77.34%, respectively.

ATR-FTIR Analysis

The spectra of aqueous and organic *Z. officinale* and the resulting ZOEE-AgNPs and ZOAE-AgNPs are shown in Figures 8 and 9 and Table 4. The *Z. officinale* (organic and aqueous) extracts and AgNPs (manufactured using *Z. officinale* organic or aqueous extracts) showed significant and minor alterations. The aqueous and organic extracts of *Z. officinale* rhizome exhibit O-H and N-H stretching of phenolic compounds, which leads to a shift in the absorption peaks from 3306.93 cm^{-1} and 3358.91 cm^{-1} to lower wavelengths of 3270.84 cm^{-1} and 3220.11 cm^{-1}, respectively. Additionally, terpenoids and saponins demonstrate characteristic absorption peaks at 2909.59 cm^{-1}, 2915.48 cm^{-1}, 2915.36 cm^{-1}, 2916.28 cm^{-1}, 2839.88 cm^{-1}, 2840.58 cm^{-1}, 2848.15 cm^{-1}, and 2848.40 cm^{-1}, indicative of aliphatic or methylene groups. Furthermore, shifts were observed for the peak at 1589.45 cm^{-1} due to the presence of alkenyl or aromatic C=C stretching, with a corresponding higher wavelength at 1631.15 cm^{-1}, and a shift for the peak at 1706.22 cm^{-1} to a lower wavelength of 1703.60 cm^{-1}. The FTIR spectrum in the 1650–1550 cm^{-1} region represents stretching of C=C, C=N, and NH, while the range of 1550–1300 cm^{-1} indicates stretching

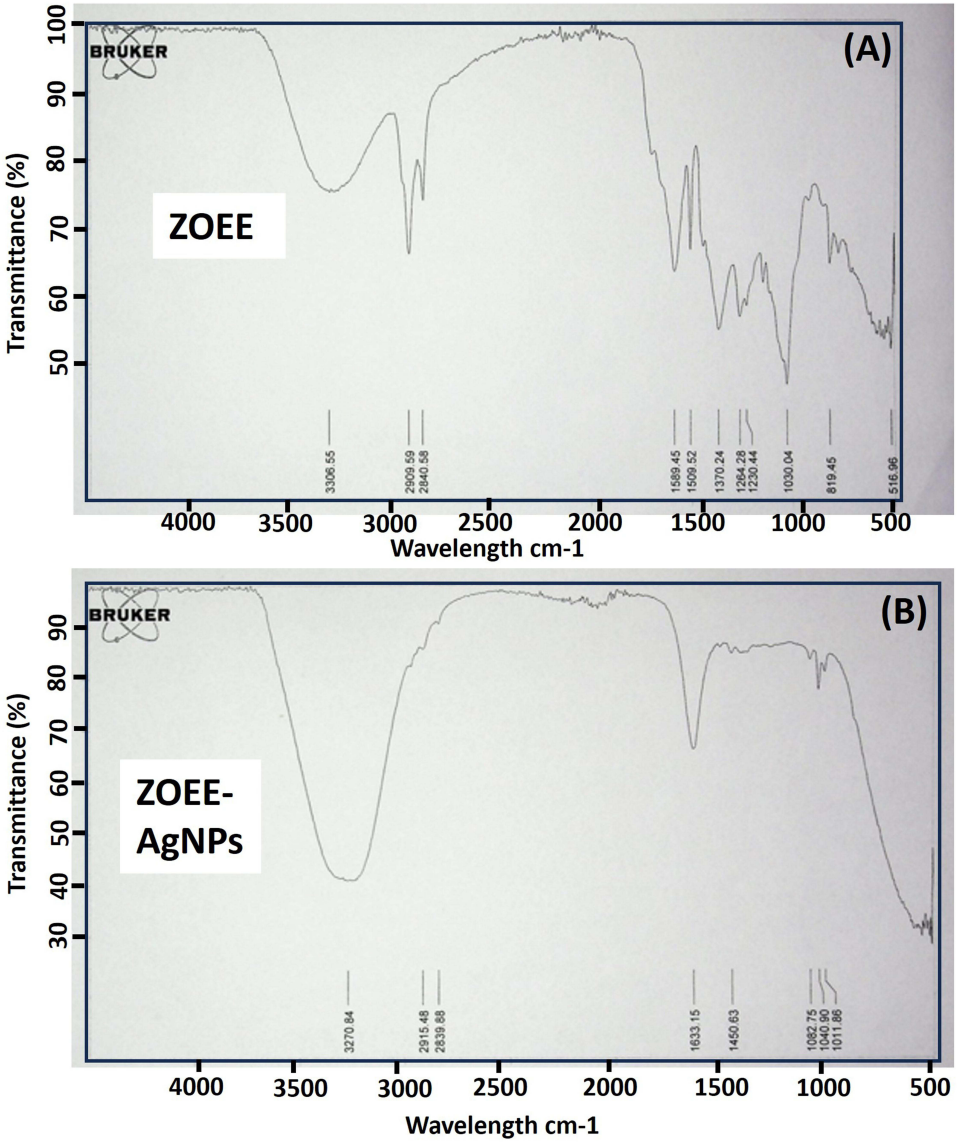

Figure 8 (**A**) ATR-FTIR for ZOEE (ZOEE-*Z. officinale* organic or ethanolic extracts). (**B**) ATR-FTIR for ZOEE-AgNPs (ZOEE-AgNPs–Biosynthesized AgNPs using *Z. officinale* organic or ethanolic extracts).

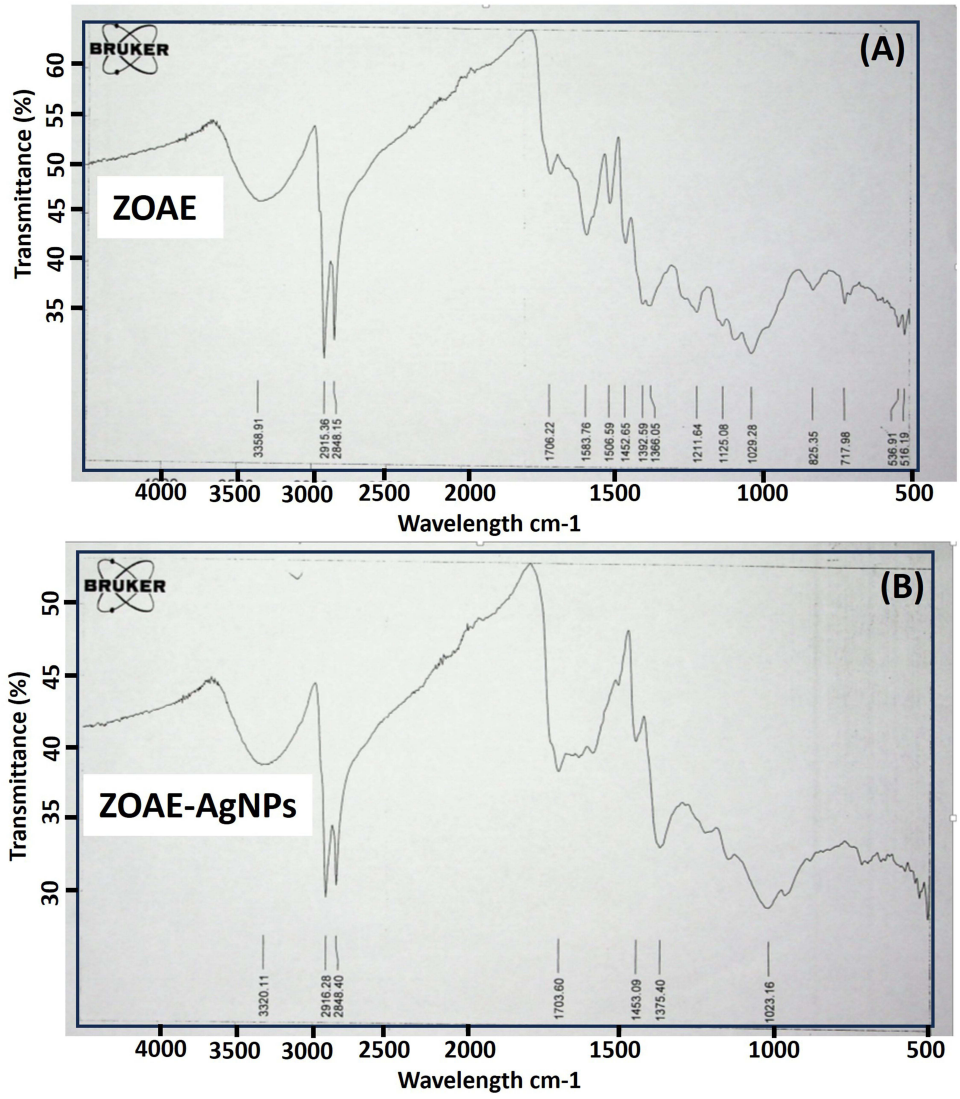

Figure 9 (**A**) ATR-FTIR for ZOAE (ZOAE-*Z. officinale* aqueous extracts). (**B**) ATR-FTIR for ZOAE-AgNPs (ZOAE-AgNPs–Biosynthesized AgNPs using *Z. officinale* aqueous extracts).

associated with NO_2 or CH_3 and CH_2 groups. The presence of C-O-C, C-OH, and P=O functional groups is suggested by peaks in the 1300–1000 cm^{-1} range. Peaks within the 800–500 cm^{-1} interval indicate the presence of aromatic compounds, while those in the 1270–650 cm^{-1} range correspond to C-H, C-O, and N-H stretching. A change in peak positions in the generated AgNPs

Table 4 Aqueous or Organic Extracts of *Z. officinale* Spectral Peak Values and Functional Groups

Wave Number Range (Detected In This Study, cm)	Wave Number Range Reference, cm	Assignment	Functional Groups	Supporting References
3270.84,3306.55, 3320.11, 3358.91	3000–3600, 3000–3500	O-H and N-H stretching	Water, alcohol, phenol, carbohydrate, peroxide	[29,40]
2909.59,2915.48,29,015.36,2916.28	2920	C-H Stretching	Polysaccharide, lipids, carbohydrates	[29]
2839.88, 2840.58, 2848.15, 2848.40	2800–2900 2850	C-H stretching	Polysaccharide, lipids, carbohydrates	[40,41]

(*Continued*)

Table 4 (Continued).

Wave Number Range (Detected In This Study, cm)	Wave Number Range Reference, cm	Assignment	Functional Groups	Supporting References
1631.15, 1706.22, 1703.60,	1600–1760	N-H binding vibration, C=O binding vibration	Amino acid, fatty acids, ester	[40,41]
1506.59, 1509.52,1583.76 1589.45,	1500–1600	Aromatic and –NH bending vibration	Amino acid	[41]
1366.05, 1370.24, 1375.40, 1392.59, 1450.83,1452.65, 1453.09	1300–1500	Primary and secondary O-H bending, and phenol	Primary, secondary and tertiary alcohol. Phenol and phenyl group	[40]
1125.08, 1211.64, 1230.44, 1264.28	1100–1270	C-O stretching vibration	Acid or ester	[40]
1011.86,1030.04, 1040.90, 1082.75	997–1130 997-1140 <1000	C-O stretching vibration CH-binding	Mono or oligosaccharide Oligosaccharide, glycoprotein Isopernoids	[40,41]

indicates that the aqueous and organic extracts of *Z. officinale* rhizome's functional group contribute to the AgNP production process. These results conflict with the phytochemical examination of the organic extracts of *Z. officinale* from the rhizome.

DLS and Zeta Potential Analysis

The size of the AgNPs synthesized biologically at pH 12 from *Z. officinale* was measured. Results from DLS showed that ZOAE-AgNPs and ZOEE-AgNPs had an average diameter of 200.5 nm and 259.2 nm, respectively, and poly dispersity (PDI) indices of 0.373 and 0.469 (Figure 10). The zeta potential of *Z. officinale* aqueous and organic extract based on biosynthesized AgNPs was −22.0 mV, −39.9 mV, ZOAE-AgNPs and ZOEE-AgNPs, respectively.

Effect of Different Physical Parameters on the Preparation of AgNPs Using Both Ginger Extracts

One milliliter of plant extracts were added into 5 mL of 10 mm silver nitrate solution for reduction into silver ions at 37°C. The physical parameters were optimized using the obtained reaction mixture of *Z. officinale* (Table 5). In this case, it was expected that maximizing SPR intensity would also produce the greatest number of NPs with smaller sizes.

Stability and Reproducibility of AgNPs

The AgNPs were tested for stability by storing the colloidal dispersion of NPs and tracking absorption spectra over time. Following a 31-day interval, the dispersion remained steady and no significant spectrum changes or precipitation were observed, indicating its stability over the examined time. More than fifteen times, the synthesis of AgNPs was carried out under ideal conditions, and each time, the characteristics were consistent.

Antimicrobial Susceptibility Test (Commercially Antibiotic)

It was found that *S. aureus* was resistant to different antibiotics. While the amoxicillin (Ax_{25}) was sensitive to *S. aureus*. Table 6 shows the sensitivity of the tested organisms to different antibiotics.

Plant Extract is Used in an Antibacterial Assay of Synthetic AgNPs Against MDR *S. aureus, Salmonella enterica* and *E. coli*

Following the application of biogenic AgNPs generated at pH 12 via particular extracts for antibiotic testing, the organisms exhibited a notable zone of inhibition (Table 3). Table 7 makes it clear that, at the same dosage of AgNPs, Gram-negative bacteria (*E. coli*) exhibit a larger zone of inhibition than Gram-positive bacteria (*S. aureus*). The observed discrepancy may

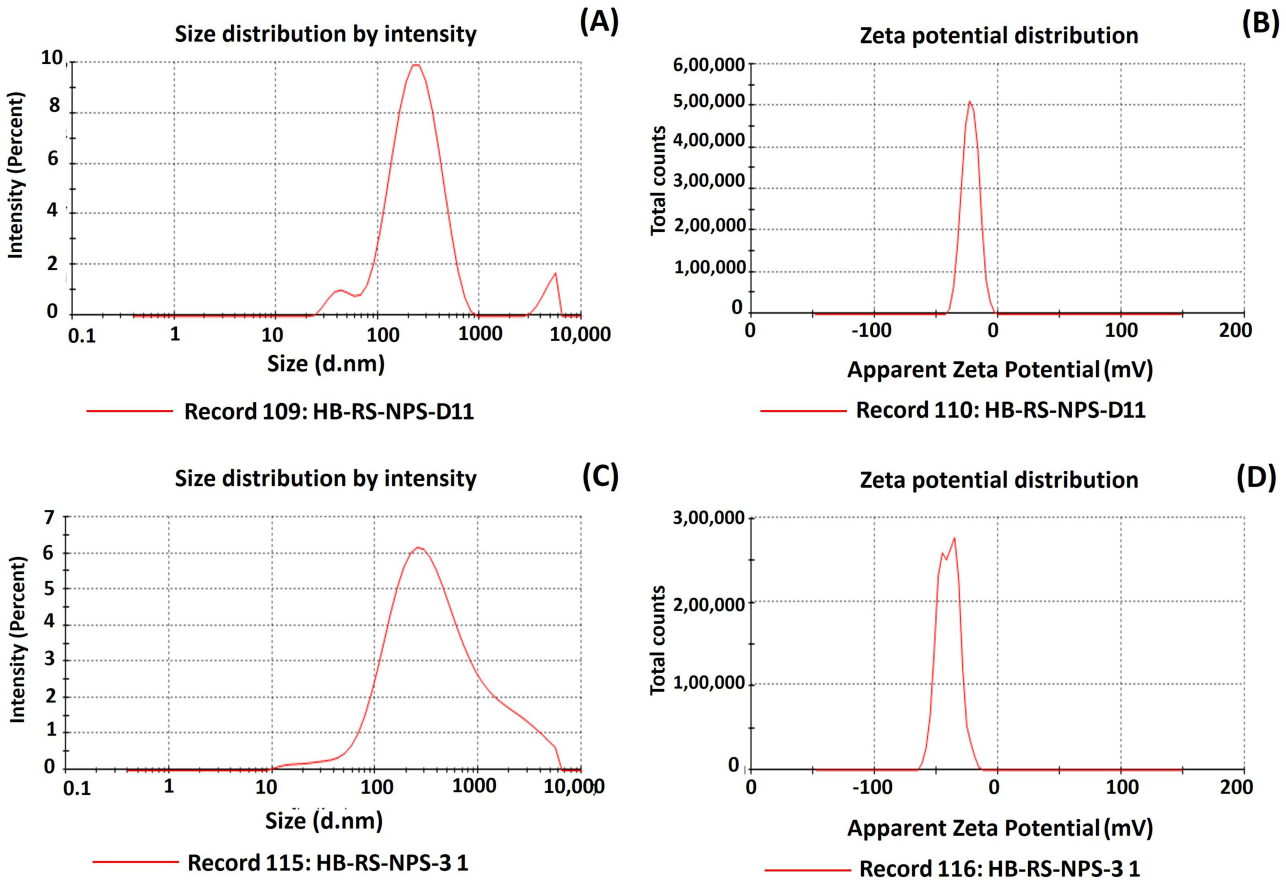

Figure 10 (**A**) Size distribution (by intensity) of ZOAE biosynthesized AgNPs. (**B**) Zeta potential distribution of ZOAE biosynthesized AgNPs. (**C**) Size distribution (by intensity) of ZOEE biosynthesized AgNPs. (**D**) Zeta potential distribution of ZOEE biosynthesized AgNPs.

be attributed to the distinct compositions of the cell walls in Gram-negative and Gram-positive bacteria. The cell wall of Gram-positive bacteria is characterized by a thick peptidoglycan layer composed of short linear polysaccharide chains cross-linked by peptides, resulting in a rigid structure that hinders the penetration of AgNPs. In contrast, the cell wall of Gram-negative bacteria features a relatively thinner peptidoglycan layer, which may facilitate easier access for AgNPs.

MIC Determination of Synthesized ZOEE-AgNPs Against *E. coli*

The minimal concentration of ZOEE-AgNPs required for the inhibition of MDR *E. coli* growth was 25 µg/mL. The minimum concentration of ZOAE-AgNPs required for the inhibition of MDR *E. coli* growth was inhibited 12.5 µg/mL.

Table 5 Summary of Different Parameter for Controlled Condition for Biosynthesized AgNPs Using Extracts of *Z. Officinale*

Optimization of Different Parameters	Corresponding Value
Temperature	37°C
pH of medium	12.0
Reaction time	24 h
Silver ion concentration	10 mm

Table 6 Bactericidal Activity Against *E. coli, Salmonella enterica* and *S. aureus*

Pathogens Species	Antibiotics	Zone of Inhibition (mm)
Escherichia coli	Amoxicillin	–
	Azocillin	–
	Cloxacillin	–
	Oxacillin	–
	Ticarcillin	–
Salmonella enterica	Amoxicillin	–
	Azocillin	–
	Cloxacillin	–
	Oxacillin	–
	Ticarcillin	–
Staphylococcus aureus	Amoxicillin	10
	Azocillin	–
	Cloxacillin	–
	Oxacillin	–
	Ticarcillin	–

Notes: Ax_{25} (Amoxicillin), Az_{75} (Azocillin), Cx_1 (Cloxacillin), Ox_1 (Oxacillin), Ti_{75} (Ticarcillin).

Table 7 Organic or Aqueous Extract of *Z. Officinale* Used to Synthesized AgNPs Showed Zone of Inhibition in Mm

Bacterial Isolates	Zone of Inhibition (mm) Means ± SD	
	ZOEE-AgNPs	ZOAE-AgNPs
Escherichia coli	18.33 ± 0.30	20.83 ± 0.53
Salmonella enterica	16.83 ± 0.47	17.33 ± 0.30
Staphylococcus aureus	13.83 ± 0.53	15.5 ± 0.50

Notes: ZOEE-AgNPs: AgNPs synthesized using *Z. officinale*. ZOAE-AgNPs: AgNPs were synthesized using the aqueous extracts *Z. officinale*.

Discussion

Biological production of NPs is an important tool for the prevention of diseases, with certain advances in nontoxic biogenic molecules (present in plant extracts) that are beneficial, cheap, and involve strategies for their assemblage.[42–44] The aim of current research was to synthesize the AgNPs using various *Z. officinale'* extracts and to evaluate how effective they were against bacteria. The conditions for preparing AgNPs were improved by the color change observed with *Z. officinale*. Within 24 h, a noticeable change in color occurred in the reaction mixture, shifting from yellow-brown to reddish-brown, indicating the synthesis of AgNPs. This transformation could be a strong indication of the reduction of silver ions to AgNPs, which is also connected to SPR.[27] In addition, the extract of *Z. officinale* and the two mixtures containing ZOAE-AgNPs and ZOEE-AgNPs were analyzed using UV-Vis spectroscopy. The factors affecting the synthesis of AgNPs were the $AgNO_3$ concentration, pH, and reaction time, which were the ratio of $AgNO_3$ to *Z. officinale'* aqueous and organic extracts. Biogenic AgNPs were generated

within a few minutes using Cetraria islandica,[27] Parmelia perlata in 30 min,[45] and Parmotrema preserediosum in 24 h.[46] It might be argued that the difference in time required for the synthesis of NPs might be linked to the type of solvent used, the method and circumstances for extraction, and the quantity of secondary metabolites in plant extracts. Our findings are consistent with those of the previous studies.[3,46–51] The UV Vis Spectra of synthesized AgNPs using ZOEE at pH 8.5 showed a maximum absorption peak at 448 nm (1.480 absorbance) for 24-hour incubation. UV Vis. Spectra synthesized AgNP using ZOEE at pH 10 or 12 also showed maximum absorbance peak 425nm (1.796 absorbance) and UV Vis. Spectra synthesized AgNP using ZOEE at pH 12 have a maximum absorbance peak of 420 nm (2.883 absorbance). Absorption intensity serves as a critical parameter for assessing the extent of NP formation, with higher absorption intensities signifying a greater concentration of NPs in solution. In contrast, at pH values of 8.5 and 10, a decrease in peak intensity was observed, which can be attributed to the agglomeration of NPs or their increased size. The first reason is an increase in pH that leads towards a reduction of distance between the particles, the homogeneity and regularity for nanomaterials or crystalline regeneration led to increased absorption and reduced transmittance. The second reason could be that higher pH is likely to provide more electrons in the reaction mixture that facilitates the overall reduction process. The alkalinity pH environment enhances the reducing and stabilizing capabilities of bioactive compounds in the plant extract.

The XRD results from the present study demonstrate that *Z. officinale*, whether derived from organic or aqueous extracts, can effectively facilitate the synthesis of Ag/AgO composite NPs. The interaction between silver ions and silver oxide ions present in the organic and aqueous extracts of *Z. officinale* is instrumental in the formation of AgO composite NPs. These findings align with prior research that has documented similar outcomes in the biosynthesis of AgNPs.[52] The XRD analysis confirmed the formation of crystalline AgNPs.[53] The peaks at 32.28°, 46. 28°, 67.47°, and 76.69° were identified in a previous study.[54]

Using ATR-FTIR, the functional groups of ZOAE or ZOEE responsible for the reduction of silver ions from $AgNO_3$ were studied, and the stabilization of AgNPs was investigated.[55] FTIR is a powerful analytical technique that allows for the identification of both organic and inorganic constituents. This provides valuable insights into the infrared spectra of solids, liquids, and gases. In order to help cap the AgNPs and identify the functional groups present in the biomolecules causing the bioreduction of Ag+, FTIR measurements were carried out. The presence of residual capping agent with the AgNPs was indicated by the FTIR spectra, which specifically showed main absorption bands at 3270.84 cm-1 and 3220.11 cm-1, 2915.48 cm-1, 2916.28 cm-1, 2839.85 cm-1, 2848.40 cm-1, 1703.60 cm-1, 1631.15 cm-1, 1450.63 cm-1 and 1453.09 cm-1, 1062.76 cm-1, 1040.90 cm-1, 1023.16 cm-1, and 1011.86 cm-1. The presence of alcohol and phenolic-related species is indicated by the large bands in the spectra of both ginger extracts that were seen at 3270.84 cm-1 and 3220.11 cm-1. These bands correspond to the O–H stretching vibration.[36,56] Four bands were found at 2915.48 cm-1, 2916.28 cm-1, 2839.85 cm-1, and 2848.40 cm-1. These bands are associated with the aromatic compound's C–H stretching. Only the ginger aqueous extract showed the tiny band at 1703.60 cm-1, which is indicative of non-conjugated C–C stretching. The bands in ginger organic extracts that occurred at 1631.15 cm-1 correspond to the C–N and C–C stretching vibrations, indicating that the presence of proteins results in amide.[27,45,55,56] The N–H stretch vibration of the amide moieties may be responsible for the two bands at 1450.63 cm-1 and 1453.09 cm-1. The four significant stretch vibrational bands found in ginger extracts (1062.76 cm-1, 1040.90 cm-1, 1023.16 cm-1, 1011.86 cm-1, and 1042 cm−1) are thought to be connected to the C–O–C stretch of polysaccharides and aromatic ethers.[40,41] It has been noted in earlier studies that these identified functional groups would probably be crucial in capping and stabilizing the as-formed AgNPs.[40,41] Primary and secondary amines and amides' –NH2 wagging is linked to the bands in the 900–600 cm−1 range. The FTIR spectroscopic finding leads to the conclusion that organic species produced from plant extracts are most likely covering the AgNPs surface.

Spherical AgNPs were confirmed by SEM-EDXA analysis. The accumulation of NPs suggests that they were in contact during stabilization. The functional groups were responsible for capping the AgNPs and were stable in size. The reduction in silver ions, as indicated by the signal produced by EDXA was 3KeV. In the range of 3keV,[57] metallic silver nanocrystals typically exhibit strong absorption spectra. Similar results have been reported in earlier studies.[46,52,54] Two impurity peaks were detected below 1KeV two impurities were detected, corresponding to carbon and oxygen, which may have arisen from the plant extract.[46,49,51] EDXA analysis of the biosynthesized AgNPs sample revealed the presence of carbon and oxygen atoms in addition to silver peaks. This provided evidence for the presence of organic chemicals, or

phytoconstituents, on the surface of biosynthesized AgNPs and supported the finding that the aqueous and organic extracts of ginger did not produce AgNPs given that plant secondary metabolites function as NPs' capping and lowering agents in addition to one another. The variations in UV Vis might be caused by the different phytoconstituent content of the organic and aqueous ginger extracts. The nanosize and spectral absorption of biosynthesised AgNPs.

DLS, which is dependent on the interaction of light with particles, was used to assess the spread of molecules between 2 and 500 nm.[58] Different characterisation techniques revealed that AgNP particle sizes are often found in the sequence DLS>XRD. AgNPs were found to be bigger in XRD than in prior studies based on DLS.[59,60] To explain this discrepancy, consider that the hydration layer, capping agents, and stabilizing operators caused the observed size to be dependent on the mix of particles and hydrodynamic radius by DLS. The results obtained from DLS in current study for ZOAE-AgNPS and ZOEE-AgNPs had an average diameter of 200.5 nm and 259.2 nm with PDI of 0.373 and 0.469.

The more homogenous the NPs, the higher the PDI, which measures the homogeneity of the NPs. The size distribution of the population within a given test sample is shown. The PDI is up to 1.0. NPs with a value less than 0.5 are regarded as sufficient for sedate transportation. In the present study, the AgNPs synthesized by *Z. officinale aqueous* and organic extract the zeta potent value was −22.0 mV for ZOAE-AgNPS and −39.9 mV for ZOEE-AgNPs in present study. Both AgNPs have negative zeta potential values, which confirms the repulsion among particles, and the negative value also shows that AgNPs are highly stable.[61]

MDR bacterial strains pose a serious threat to public health and have been reported worldwide. *S. aureus* is among the multidrug resistant species of bacteria whose antibacterial susceptibility to AgNPs has been previously reported in various studies.[22,40,48,62,63] It is possible that the antimicrobial properties of AgNPs originate from their components. Some important enzymes, thiol groups, and silver ions participate in powerful processes, ultimately making them inactive.

The study's findings demonstrate the value of synthesized AgNPs in combating strains of *Salmonella enterica, E. coli*, and *S. aureus*. AgNPs produced from green materials substantially reduced *S. aureus, E. coli*, and *Salmonella enterica*. In previous studies, AgNPs have been shown to possess the ability to combat various bacterial species, including those that are extensively drug resistant (XDR).[64,65] AgNPs have been found to be highly effective antibacterial agents.[66] In another study, NPs derived from *S. potatorum* leaf extract demonstrated efficacy against *S. aureus*.[67] Antimicrobial efficacy of AgNPs prepared from organic and aqueous extracts of *Z. officinale* against MDR bacteria.[68] The dense peptidoglycan layer of Gram-positive bacterial cell walls, made of straight polysaccharide chains cross-linked by peptides, creates a stronger framework that prevents the interaction of AgNPs.[69] There is a suggested mechanism for the AgNP action against microbial pathogens, such as *E. coli* and *S. aureus*. According to this process, when AgNPs come into contact with water or tissue fluid, silver ions are released. The electron donor functional groups, such as phosphates, thiols, and indoles, which include sulfur and phosphorous compounds, were bound by the silver ions after they had pierced the cell membrane. Since each of these substances is found in ribosomes or DNA, the function of the DNA was thrown off, preventing DNA replication. The microbial cell was unable to expand as a consequence, and it finally perished.

Different MIC values have been reported in previous studies. Because the antibacterial activity of AgNPs cannot be measured using a single method, researchers have employed different techniques to compare the results because it is challenging.[70]

Study limitations and future direction

Although the current study has thoroughly investigated the NPs synthesized from ginger extracts, there are certain limitations of the study which could be considered for further future studies. In the current study, we were not able to countercheck the characterization of AgNPs using more recent techniques such as Transmission electron microscopy, thermogravimetric analysis, X-ray photoelectron spectroscopy, which can provide a more comprehensive understanding of the NP properties. Furthermore, the future studies could be strengthened by including additional antimicrobial tests such as time-kill assays or biofilm inhibition studies.

Conclusion

In conclusion, the organic and aqueous extracts of ginger showed great capability to synthesize AgNPs. UV-Vis absorption peak at 420 nm for ZOEE and 425 nm clearly indicated the formation of AgNPs. XRD patterns confirmed

the phase composition and nature of synthesized NPs. ATR-FTIR spectroscopy studies confirmed the formation of AgNPs by the action of different phytochemicals with their different functional groups present in plant extract solution. SEM imaging revealed the remarkable potential for further applications of these NPs owing to their distinct spherical shape. EDX spectra confirmed the presence of elemental signals in AgNPs. The green synthesis of AgNPs is cost-effective, safe, nontoxic, and an eco-friendly approach for mass production, as well as having potential against MDR bacterial strains. Significant antibacterial activity was shown by AgNPs against *Escherichia coli* compared to *Staphylococcus aureus,* which concluded that the AgNPs were more effective against Gram negative bacteria. These NPs have the potential to offer their application in biomedical and related fields to improve the quality of life. With the advancement of research in this field, the use of biosynthetic AgNPs could potentially offer more benefits than the conventional chemical synthesis methods. This has led to exciting advancements in various industries.

Institutional Review Board Statement

The Human Research Ethics Committee, Faculty of Life Sciences, University of Central Punjab, Lahore, Pakistan, granted ethical permission for the research, which was carried out in accordance with the Declaration of Helsinki. The code for the committee's approval is HREC UCP Code: CP/FOLS/210419-6.

Acknowledgments

Naveed Ahmed would like to acknowledge the USM research assistance scheme of Universiti Sains Malaysia.

Disclosure

The authors report no conflicts of interest in this work.

References

1. Hamzeh M, Sunahara GI. In vitro cytotoxicity and genotoxicity studies of titanium dioxide (TiO2) nanoparticles in Chinese hamster lung fibroblast cells. *Toxicol in vitro*. 2013;27(2):864–873. doi:10.1016/j.tiv.2012.12.018
2. Assad N, Naeem-ul-Hassan M, Ajaz Hussain M, et al. Diffused sunlight assisted green synthesis of silver nanoparticles using Cotoneaster nummularia polar extract for antimicrobial and wound healing applications. *Nat Prod Res*;2023. 1–15. doi:10.1080/14786419.2023.2295936
3. Khalil MM, Ismail EH, El-Baghdady KZ, Mohamed D. Green synthesis of silver nanoparticles using olive leaf extract and its antibacterial activity. *Arabian J Chem*. 2014;7(6):1131–1139. doi:10.1016/j.arabjc.2013.04.007
4. Balaraman P, Balasubramanian B, Kaliannan D, et al. Phyco-synthesis of silver nanoparticles mediated from marine algae Sargassum myriocystum and its potential biological and environmental applications. *Waste Biomass Valorization*. 2020;11:5255–5271. doi:10.1007/s12649-020-01083-5
5. Ejaz A, Mamtaz Z, Yasmin I, et al. Cyperus scariosus extract based greenly synthesized gold nanoparticles as colorimetric nanoprobe for Ni2+ detection and as antibacterial and photocatalytic agent. *J Mol Liq*. 2024;393:123622. doi:10.1016/j.molliq.2023.123622
6. Preethi R, Padma P. Anticancer activity of silver nanobioconjugates synthesized from Piper betle leaves extract and its active compound eugenol. *Int J Pharm Pharm Sci*. 2016;8(9):201–205. doi:10.22159/ijpps.2016.v8i9.12993
7. Khan AW, Lali NS, Sabei FY, et al. Sunlight-assisted green synthesis of gold nanocubes using horsetail leaf extract: a highly selective colorimetric sensor for Pb2+, photocatalytic and antimicrobial agent. *J Environ Chem Eng*. 2024;12(3):112576. doi:10.1016/j.jece.2024.112576
8. Rauwel P, Rauwel E, Ferdov S, Singh MP. Silver nanoparticles: synthesis, properties, and applications. *Adv Mater Sci Eng*. 2015;2015:1–2.
9. Cyril N, George JB, Joseph L, Raghavamenon A, S VP. Assessment of antioxidant, antibacterial and anti-proliferative (lung cancer cell line A549) activities of green synthesized silver nanoparticles from Derris trifoliata. *Toxicol Res*. 2019;8(2):297–308. doi:10.1039/C8TX00323H
10. Gheisari F, Kasaee SR, Mohamadian P, et al. Bromelain-loaded silver nanoparticles: formulation, characterization and biological activity. *Inorg Chem Commun*. 2024;161:112006. doi:10.1016/j.inoche.2023.112006
11. Parveen S, Saqib S, Ahmed A, Shahzad A, Ahmed N. Prevalence of MRSA colonization among healthcare-workers and effectiveness of decolonization regimen in ICU of a tertiary care hospital, Lahore, Pakistan. *Adv Life Sci*. 2020;8(1):38–41.
12. Ricke SC, Hacker JC, Yearkey KL, Shi Z, Park SH, Rainwater CE. Unraveling food production microbiomes: concepts and future directions. *Food Feed Safety Sys Ana*. 2018;2018:347–374
13. Hiremath J, Rathod V, Ninganagouda S, Singh D, Prema K. Antibacterial activity of silver nanoparticles from *Rhizopus spp*. against gram negative *E. coli* MDR strains. *J Pure Appl Microbiol*. 2014;8(1):555–562.
14. Tariq F, Ahmed N, Afzal M, Khan MAU, Synthesis ZB. Characterization and antimicrobial activity of *Bacillus subtilis*-derived silver nanoparticles against multidrug-resistant bacteria. *Jundishapur J Microbiol*. 2020;13(5). doi:10.5812/jjm.91934
15. Heboyan A, Manrikyan M, Zafar MS, et al. Bacteriological evaluation of gingival crevicular fluid in teeth restored using fixed dental prostheses: an in vivo study. *Int J Mol Sci*. 2021;22(11):5463. doi:10.3390/ijms22115463
16. Banerjee P, Satapathy M, Mukhopahayay A, Das P. Leaf extract mediated green synthesis of silver nanoparticles from widely available Indian plants: synthesis, characterization, antimicrobial property and toxicity analysis. *Biores Bioproc*. 2014;1(1):1–10. doi:10.1186/s40643-014-0003-y
17. Aziz S B, Hussein G, Brza M, et al. Fabrication of interconnected plasmonic spherical silver nanoparticles with enhanced localized surface plasmon resonance (LSPR) peaks using quince leaf extract solution. *Nanomaterials*. 2019;9(11):1557. doi:10.3390/nano9111557

18. Bhuiyan MNI, Chowdhury JU, Begum J. Chemical investigation of the leaf and rhizome essential oils of *Zingiber zerumbet* (L.) Smith from Bangladesh. *Bangladesh J Pharmacol*. 2009;4(1):9–12.
19. Lal V, Pandey A, Tripathi P, Pandey R. Insignificant antidiabetic activity of rhizome of *Zingiber zerumbet*. *J Pharma Negative Res*. 2010;1(2):58–60.
20. Haider A, Ijaz M, Ali S, et al. Green synthesized phytochemically (*Zingiber officinale* and *Allium sativum*) reduced nickel oxide nanoparticles confirmed bactericidal and catalytic potential. *Nanoscale Res Lett*. 2020;15(1):1–11. doi:10.1186/s11671-020-3283-5
21. Prasad S, Tyagi AK. Ginger and its constituents: role in prevention and treatment of gastrointestinal cancer. *Gastroenterol Res Pract*. 2015;2015:1–11. doi:10.1155/2015/142979
22. Lal V, Tripathi P, Pandey RD, Lal VK. Insignificant antidiabetic activity of rhizome of Zingiber zerumbet. *J Pharma Negative Res*. 2010;1(2):58–60. doi:10.4103/0976-9234.75707
23. Jabbar A, Abbas A, Assad N, et al. A highly selective Hg 2+ colorimetric sensor and antimicrobial agent based on green synthesized silver nanoparticles using Equisetum diffusum extract. *RSC Adv*. 2023;13(41):28666–28675. doi:10.1039/D3RA05070J
24. Anand K, Gengan R, Phulukdaree A, Chuturgoon A. Agroforestry waste Moringa oleifera petals mediated green synthesis of gold nanoparticles and their anti-cancer and catalytic activity. *J Ind Eng Chem*. 2015;21:1105–1111. doi:10.1016/j.jiec.2014.05.021
25. Mradu G, Saumyakanti S, Sohini M, Arup M. HPLC profiles of standard phenolic compounds present in medicinal plants. *IntJ Pharmacogn Phytochem Res*. 2012;4(3):162–167.
26. Sultana B, Anwar F. Flavonols (kaempeferol, quercetin, myricetin) contents of selected fruits, vegetables and medicinal plants. *Food Chem*. 2008;108(3):879–884. doi:10.1016/j.foodchem.2007.11.053
27. Yıldız N, Ateş Ç, Yılmaz M, Demir D, Yıldız A, Çalımlı A. Investigation of lichen based green synthesis of silver nanoparticles with response surface methodology. *Green Processing Synthesis*. 2014;3(4):259–270. doi:10.1515/gps-2014-0024
28. Jamdagni P, Khatri P, Rana J-S. Green synthesis of zinc oxide nanoparticles using flower extract of Nyctanthes arbor-tristis and their antifungal activity. *J King Saud Univ Sci*. 2018;30(2):168–175. doi:10.1016/j.jksus.2016.10.002
29. Ramzan M, Karobari MI, Heboyan A, et al. Synthesis of silver nanoparticles from extracts of wild ginger (Zingiber zerumbet) with antibacterial activity against selective multidrug resistant oral bacteria. *Molecules*. 2022;27(6):2007. doi:10.3390/molecules27062007
30. Swamy MK, Akhtar MS, Mohanty SK, Sinniah UR. Synthesis and characterization of silver nanoparticles using fruit extract of Momordica cymbalaria and assessment of their in vitro antimicrobial, antioxidant and cytotoxicity activities. *Spectrochimica Acta, Part A*. 2015;151:939–944. doi:10.1016/j.saa.2015.07.009
31. Govindappa M, Channabasava R, Kumar KS, Pushpalatha K. Antioxidant activity and phytochemical screening of crude endophytes extracts of Tabebuia argentea Bur. & K. Sch. *Am J Plant Sci*. 2013;2013:1.
32. Bhakya S, Muthukrishnan S, Sukumaran M, Muthukumar M. Biogenic synthesis of silver nanoparticles and their antioxidant and antibacterial activity. *Appl. Nanosci*. 2016;6(5):755–766. doi:10.1007/s13204-015-0473-z
33. Sreelekha E, George B, Shyam A, Sajina N, Mathew B. A comparative study on the synthesis, characterization, and antioxidant activity of green and chemically synthesized silver nanoparticles. *BioNanoScience*. 2021;11(2):489–496. doi:10.1007/s12668-021-00824-7
34. Ahmad A, Wei Y, Syed F, et al. Isatis tinctoria mediated synthesis of amphotericin B-bound silver nanoparticles with enhanced photoinduced antileishmanial activity: a novel green approach. *J Photochem Photobiol B Biol*. 2016;161:17–24. doi:10.1016/j.jphotobiol.2016.05.003
35. Ahmad A, Syed F, Shah A, et al. Silver and gold nanoparticles from Sargentodoxa cuneata: synthesis, characterization and antileishmanial activity. *RSC Adv*. 2015;5(90):73793–73806. doi:10.1039/C5RA13206A
36. Siddiqi KS, Rashid M, Rahman A, et al. Biogenic fabrication and characterization of silver nanoparticles using aqueous-ethanolic extract of lichen (Usnea longissima) and their antimicrobial activity. *Biomater Res*. 2018;22(1):23. doi:10.1186/s40824-018-0135-9
37. Wayne P. Clinical and laboratory standards institute. *Perform Standards Antimicrobial Susceptibility Testing*. 2011;2011:1.
38. Altaf M, Ijaz M, Ghaffar A, Rehman A, Avais M. Antibiotic susceptibility profile and synergistic effect of non-steroidal anti-inflammatory drugs on antibacterial activity of resistant antibiotics (Oxytetracycline and Gentamicin) against methicillin resistant Staphylococcus aureus (MRSA). *Microb Pathogenesis*. 2019;137:103755. doi:10.1016/j.micpath.2019.103755
39. Omara ST, Abd El-Moez I, Mohamed M. Antibacterial effect of Origanum majorana L.(marjoram) and Rosmarinus officinalis L.(rosemary) essential oils on food borne pathogens isolated from raw minced meat in Egypt. *Glob Vet*. 2014;13(6):1056–1064.
40. Caunii A, Pribac G, Grozea I, Gaitin D, Samfira I. Design of optimal solvent for extraction of bio–active ingredients from six varieties of Medicago sativa. *Chem Cent J*. 2012;6(1):1–8. doi:10.1186/1752-153X-6-123
41. Topalăa CM Tătarua LD. ATR-FTIR spectra fingerprinting of medicinal herbs extracts prepared using microwave extraction. *Arabian J Med Aromatic Plants*. 2017;3(1):1–9.
42. Veerasamy R, Xin TZ, Gunasagaran S, et al. Biosynthesis of silver nanoparticles using mangosteen leaf extract and evaluation of their antimicrobial activities. *J Saudi Chem Soc*. 2011;15(2):113–120. doi:10.1016/j.jscs.2010.06.004
43. Shah A, Akhtar S, Mahmood F, et al. Fagonia arabica extract-stabilized gold nanoparticles as a highly selective colorimetric nanoprobe for Cd2+ detection and as a potential photocatalytic and antibacterial agent. *Surf Interfaces*. 2024;51:104556. doi:10.1016/j.surfin.2024.104556
44. Ullah S, Khalid R, Rehman MF, et al. Biosynthesis of phyto-functionalized silver nanoparticles using olive fruit extract and evaluation of their antibacterial and antioxidant properties. *Front Chem*. 2023;11:1202252. doi:10.3389/fchem.2023.1202252
45. Leela K, Anchana DC. A study on the applications of silver nanoparticle synthesized using the aqueous extract and the purified secondary metabolites of lichen Parmelia perlata. *Int J Pharm Sci Invention*. 2017;6(10):42–59.
46. Mie R, Samsudin MW, Din LB, Ahmad A, Ibrahim N, Adnan SNA. Synthesis of silver nanoparticles with antibacterial activity using the lichen Parmotrema praesorediosum. *Int j Nanomed*. 2014;9:121–127. doi:10.2147/IJN.S52306
47. Amruthraj NJ, Preetam Raj JP, Lebel A. Capsaicin-capped silver nanoparticles: its kinetics, characterization and biocompatibility assay. *Appl. Nanosci*. 2015;5:403–409. doi:10.1007/s13204-014-0330-5
48. Chung I-M, Park I, Seung-Hyun K, Thiruvengadam M, Rajakumar G. Plant-mediated synthesis of silver nanoparticles: their characteristic properties and therapeutic applications. *Nanoscale Res Lett*. 2016;11:1–14. doi:10.1186/s11671-016-1257-4
49. Din LB, Mie R, Samsudin MW, Ahmad A, Ibrahim N. Biomimetic synthesis of silver nanoparticles using the lichen Ramalina dumeticola and the antibacterial activity. *Malays J Anal Sci*. 2015;19:369–376.

50. Iravani S, Zolfaghari B. Green synthesis of silver nanoparticles using Pinus eldarica bark extract. *Biomed Res Int*. 2013;2013:1–5. doi:10.1155/2013/639725
51. Paul S, Singh AR, Sasikumar CS. Green synthesis of bio-silver nanoparticles by Parmelia perlata, Ganoderma lucidum and Phellinus igniarius & their fields of application. *Indian J Res Pharm Biotechnol*. 2015;3(2):100.
52. Kumar VA, Uchida T, Mizuki T, et al. Synthesis of nanoparticles composed of silver and silver chloride for a plasmonic photocatalyst using an extract from a weed Solidago altissima (goldenrod). *Adv Nat Sci*. 2016;7(1):015002.
53. Kumar V, Yadav SK. Plant-mediated synthesis of silver and gold nanoparticles and their applications. *J Chem Technol Biotechnol Int Res Process Environ Clean Technol*. 2009;84(2):151–157. doi:10.1002/jctb.2023
54. Jeeva K, Thiyagarajan M, Elangovan V, Geetha N, Venkatachalam P. Caesalpinia coriaria leaf extracts mediated biosynthesis of metallic silver nanoparticles and their antibacterial activity against clinically isolated pathogens. *Ind Crops Prod*. 2014;52:714–720. doi:10.1016/j.indcrop.2013.11.037
55. Khandel P, Kumar Shahi S, Kanwar L, Kumar Yadaw R, Kumar Soni D. Biochemical profiling of microbes inhibiting Silver nanoparticles using symbiotic organisms. *Int J Nano Dimension*. 2018;9(3):273–285.
56. Dasari S, Suresh K, Rajesh M, et al. Biosynthesis, characterization, antibacterial and antioxidant activity of silver nanoparticles produced by lichens. *J Bionanosci*. 2013;7(3):237–244. doi:10.1166/jbns.2013.1140
57. Wang C, Kim YJ, Singh P, Mathiyalagan R, Jin Y, Yang DC. Green synthesis of silver nanoparticles by Bacillus methylotrophicus, and their antimicrobial activity. *Artif Cells Nanomed Biotechnol*. 2016;44(4):1127–1132. doi:10.3109/21691401.2015.1011805
58. Taraschewski M, Cammenga H, Tuckermann R, Bauerecker S. FTIR study of CO2 and H2O/CO2 nanoparticles and their temporal evolution at 80 K. *J Phys Chem A*. 2005;109(15):3337–3343. doi:10.1021/jp044075r
59. Danaei M, Dehghankhold M, Ataei S, et al. Impact of particle size and polydispersity index on the clinical applications of lipidic nanocarrier systems. *Pharmaceutics*. 2018;10(2):57. doi:10.3390/pharmaceutics10020057
60. Ezealisiji K, Noundou X, Ukwueze S. Green synthesis and characterization of monodispersed silver nanoparticles using root bark aqueous extract of Annona muricata Linn and their antimicrobial activity. *Appl. Nanosci* 2017;7:905–911. doi:10.1007/s13204-017-0632-5
61. Bélteky P, Rónavári A, Igaz N, et al. Silver nanoparticles: aggregation behavior in biorelevant conditions and its impact on biological activity. *Int j Nanomed*. 2019;Volume 14:667–687. doi:10.2147/IJN.S185965
62. Loo YY, Chieng BW, Nishibuchi M, Radu S. Synthesis of silver nanoparticles by using tea leaf extract from Camellia sinensis. *Int j Nanomed*. 2012;2012:4263–4267.
63. Tang T, Gao Q, Barrow P, et al. Development and evaluation of live attenuated Salmonella vaccines in newly hatched duckings. *Vaccine*. 2015;33(42):5564–5571. doi:10.1016/j.vaccine.2015.09.004
64. Boonkaew B, Kempf M, Kimble R, Supaphol P, Cuttle L. Antimicrobial efficacy of a novel silver hydrogel dressing compared to two common silver burn wound dressings: acticoat™ and PolyMem Silver®. *Burns*. 2014;40(1):89–96. doi:10.1016/j.burns.2013.05.011
65. Patil S, Desai N, Mahadik K, Paradkar A. Can green synthesized propolis loaded silver nanoparticulate gel enhance wound healing caused by burns? *Eur J Int Med*. 2015;7(3):243–250. doi:10.1016/j.eujim.2015.03.002
66. Raman G, Park SJ, Sakthivel N, Suresh AK. Physico-cultural parameters during AgNPs biotransformation with bactericidal activity against human pathogens. *Enzyme Microb Technol*. 2017;100:45–51. doi:10.1016/j.enzmictec.2017.02.002
67. Kagithoju S, Godishala V, Nanna RS. Eco-friendly and green synthesis of silver nanoparticles using leaf extract of Strychnos potatorum Linn. F. and their bactericidal activities. *3 Biotech*. 2015;5:709–714. doi:10.1007/s13205-014-0272-3
68. Savithramma N, Rao ML, Devi PS. Evaluation of antibacterial efficacy of biologically synthesized silver nanoparticles using stem barks of Boswellia ovalifoliolata Bal. and Henry and Shorea tumbuggaia Roxb. 2011.
69. Singhal G, Bhavesh R, Kasariya K, Sharma AR, Singh RP. Biosynthesis of silver nanoparticles using Ocimum sanctum (Tulsi) leaf extract and screening its antimicrobial activity. *J Nanopart Res*. 2011;13:2981–2988. doi:10.1007/s11051-010-0193-y
70. Zarei M, Jamnejad A, Khajehali E. Antibacterial effect of silver nanoparticles against four foodborne pathogens. *Jundishapur J Microbiol*. 2014;7(1). doi:10.5812/jjm.8720